

# Sticky “Delivering-From” Strategies Using Viral Vectors for Efficient Human Neural Stem Cell Infection by Bioinspired Catecholamines

Eunmi Kim,<sup>†</sup> Slgirim Lee,<sup>†</sup> Seonki Hong,<sup>‡</sup> Gyuhung Jin,<sup>†</sup> Minhee Kim,<sup>†</sup> Kook In Park,<sup>§</sup> Haeshin Lee,<sup>‡</sup> and Jae-Hyung Jang<sup>\*†</sup>

<sup>†</sup>Department of Chemical and Biomolecular Engineering, Yonsei University, 50 Yonsei-Ro, Seoul 120-749, Korea

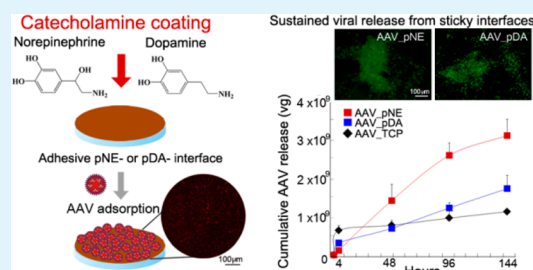
<sup>‡</sup>Department of Chemistry, Korea Advanced Institute of Science and Technology (KAIST), Daejeon 305-701, Korea,

<sup>§</sup>Department of Pediatrics, College of Medicine, Yonsei University, 50 Yonsei-Ro, Seoul 120-749, Korea

## S Supporting Information

**ABSTRACT:** Controlled release of biosuprstructures, such as viruses, from surfaces has been a challenging task in providing efficient ex vivo gene delivery. Conventional controlled viral release approaches have demonstrated low viral immobilization and burst release, inhibiting delivery efficiency. Here, a highly powerful substrate-mediated viral delivery system was designed by combining two key components that have demonstrated great potential in the fields of gene therapy and surface chemistry, respectively: adeno-associated viral (AAV) vectors and adhesive catecholamine surfaces. The introduction of a nanoscale thin coating of catecholamines, poly(norepinephrine) (pNE) or poly(dopamine) (pDA) to provide AAV adhesion followed by human neural stem cell (hNSC) culture on sticky solid surfaces exhibited unprecedented results: approximately 90% loading vs 25% (AAV\_bare surface), no burst release, sustained release at constant rates, approximately 70% infection vs 20% (AAV\_bare surface), and rapid internalization. Importantly, the sticky catecholamine-mediated AAV delivery system successfully induced a physiological response from hNSCs, cellular proliferation by a single-shot of AAV encoding fibroblast growth factor-2 (FGF-2), which is typically achieved by multiple treatments with expensive FGF-2 proteins. By combining the adhesive material-independent surface functionalization characters of pNE and pDA, this new sticky “delivering-from” gene delivery platform will make a significant contribution to numerous fields, including tissue engineering, gene therapy, and stem cell therapy.

**KEYWORDS:** substrate-mediated gene delivery, adeno-associated virus, poly(norepinephrine), poly(dopamine), neural stem cells, sticky interfaces



## 1. INTRODUCTION

Gene delivery technology plays a pivotal role in elucidating a variety of biological events observed in many areas of stem cell biology, gene therapy, and tissue engineering. Thus, developing systems that are capable of efficiently delivering genes of interest to clinically valuable cell types, such as cancer or stem cells, is critical for improving the therapeutic potential of gene delivery. In most in vitro or ex vivo cases, gene vectors are directly added to a medium (i.e., the “delivering-to” approach), and they passively diffuse into the cellular membrane for subsequent cellular uptake. In contrast, substrate-mediated delivery (i.e., the “delivering-from” approach) is based on the immobilization of gene vectors on biomaterial surfaces prior to cellular adhesion, thereby reversing the delivery direction.<sup>1,2</sup> Immobilizing gene delivery vectors onto substrates directly places the vectors into cellular microenvironments, dramatically enhancing the efficiency of gene transfer by temporally increasing physical contacts between target cells and gene vectors.<sup>3</sup> Additionally, the “delivering-from” strategy avoids exposing gene vectors to harsh processes (e.g., organic solvent exposure), as gene vectors adhere to completely formulated

structures.<sup>1</sup> Because of these advantages, advancing a new platform for “delivering-from” systems is critical for numerous biomedical applications.

Existing “delivering-from” approaches have primarily focused on nonviral systems due to their ease of chemical or physical modification to promote intimate interactions with biomaterial substrates.<sup>4–6</sup> Functionalization of biomaterial surfaces facilitated the immobilization of nonviral vectors, which led to the localization of gene expression with enhanced delivery efficiencies.<sup>7,8</sup> However, their low delivery efficiency compared to viral vector limited the advancement of “delivering-from” systems. Thus, the development of an efficient “delivering-from” strategy utilizing viral vectors remains a critical challenge.<sup>1</sup> The following are the most common methods for surface immobilization of viral vectors: physical adsorption,<sup>9,10</sup> introduction of an affinity tag on the exterior of the virus,<sup>11,12</sup> and formulation of self-assembled monolayers.<sup>13</sup> In general,

Received: February 22, 2014

Accepted: May 15, 2014

Published: May 15, 2014

these approaches may suffer problems related to the immobilization stability of gene vectors on surfaces, initial burst release, complicated steps for virus-engineering, and timely or laborious processes.

Therefore, successful development of a next generation approach that can bypass sophisticated molecular biology procedures or surface chemistry and can stably immobilize viruses of interest in surfaces will increase the prominence of the “delivering-from” strategy. Thus, we hypothesized that formulating adhesive surfaces that are compatible with viruses can solve the aforementioned challenges by attenuating the rapid dissociation of viral vectors from surfaces, avoiding DNA-level virus-engineering, and simplifying the surface modification step. To address these challenges, we chose the adhesive catecholamines poly(dopamine)(pDA)<sup>14</sup> and poly-(norepinephrine)(pNE)<sup>15,16</sup> as new platforms for the “delivering-from” strategy for viral vectors. A specialized AAV vector, AAVr3.45, which was genetically engineered through directed evolution to target neural stem cells,<sup>17</sup> was stably adhered onto pNE or pDA sticky interfaces. Human neural stem cells (hNSCs) were subsequently cultured onto the surfaces. The sticky characteristics resulted in AAV vectors displaying high loading, stable immobilization, and sustained release without burst. The functionalized surface induced rapid viral internalization and significantly enhanced gene delivery compared to the “delivering-to” approach. These sticky interface-mediated systems stimulated hNSC proliferation, further demonstrating their potential for ex vivo applications. This study represents a completely new direction for catecholamine research that extends to the delivery of supramolecules exemplified as viral vectors, whereas existing applications have focused on the functionalization of biointerfaces and material sciences such as mammalian cell adhesion,<sup>18,19</sup> hydroxyapatite formation,<sup>20</sup> the production of antibacterial surfaces,<sup>21</sup> microfluidics,<sup>22</sup> encapsulations,<sup>23</sup> lithium-ion battery production,<sup>24</sup> and the synthesis of conducting, carbonaceous films.<sup>25</sup>

## 2. EXPERIMENTAL SECTION

**2.1. Cell Culture.** To package AAV vectors, AAV293 cells (Stratagene, La Jolla, CA, USA) that were genetically engineered for AAV production were cultured in Dulbecco's modified Eagle's medium (DMEM; Invitrogen, Carlsbad, CA, USA) with 10% fetal bovine serum (FBS) (Invitrogen) and 1% penicillin and streptomycin (Invitrogen) at 37 °C and 5% CO<sub>2</sub>. To quantify cellular transduction, human neural stem cells (hNSCs) derived from the telencephalon (HFT13)<sup>26</sup> were cultured in DMEM/F12 (Invitrogen) containing N-2 supplement, 20 ng/mL of fibroblast growth factor-2 (FGF-2; Invitrogen), 8 μg/mL of heparin (Sigma-Aldrich, St. Louis, MO, USA), and 10 ng/mL of leukemia inhibitory factor (LIF; Chemicon, Temecula, CA, USA). Every 7–10 days, cells were split into fresh dishes by mechanical dissociation after trypsin treatment. To confirm enhanced gene delivery efficiencies on the sticky interfaces, additional adherent cell type, human embryonic kidney cell line (HEK293T), was cultured in DMEM with 10% FBS (Invitrogen) and 1% penicillin and streptomycin (Invitrogen) at 37 °C and 5% CO<sub>2</sub>.

**2.2. Production of AAV Vectors.** A specialized AAV vector (AAVr3.45) that was engineered to specifically target neural stem cells by directed evolution in a previous study<sup>17</sup> was used as a gene delivery vehicle in this study. The AAVr3.45 capsid contains an insertion [LATQVGQKTA (wt AAV2:583 LQRGNRQA-)] at amino acid (aa) 587 and an additional V719M mutation. Recombinant AAVr3.45 vectors carrying cDNA coding for green fluorescent protein (GFP) driven by a cytomegalovirus (CMV) promoter were packaged using transient transfection.<sup>27</sup> Briefly, equal masses (17 μg) of three plasmids, an AAV helper plasmid carrying cap r3.45 gene (pAAV

r3.45), a CMV GFP vector plasmid containing the inverted terminal repeat (ITR) (pAAV CMV GFP), and an adenoviral helper plasmid (Stratagene), were complexed in calcium phosphate solution and subsequently transfected into AAV 293 cells. At 2 days post-transfection, the resulting viral vectors were harvested and purified using a 1-mL HiTrap heparin column (GE Healthcare, Pittsburgh, PA, USA), according to the manufacturer's instructions. The eluted solution was desalted and buffer-exchanged into PBS/0.01% Tween 20 using Amicon Ultra-15 centrifugal filter units (Millipore, Billerica, MA, USA). Finally, viral genomic DNA was extracted from DNase-resistant particles, and the genomic titers were determined by quantitative PCR (qPCR) (Mini Opticon, Bio-Rad, Hercules, CA, USA) using a SYBR Green probe.

### 2.3. Generation of Adhesive Substrate Using pNE or pDA.

Prior to AAV adsorption, tissue culture polystyrene (TCP) surfaces were coated with pNE or pDA. Initially, L-(–)-norepinephrine or L-dopamine was dissolved in 10 mM Tris (pH 8.5) at various concentrations (2 and 0.02 mg/mL). Subsequently, 200 μL of each solution was directly dropped onto the TCP surfaces (48-well plate) and gently agitated at room temperature for 12 h. During this incubation step, norepinephrine or dopamine monomers were polymerized to generate adhesive pNE or pDA interfaces on the TCP surfaces.<sup>14,15</sup> The coated substrates were rinsed twice with PBS solution containing 0.01% Tween 20 (Sigma-Aldrich) to remove barely adsorbed pNE or pDA residues. An unmodified TCP surface served as a control.

**2.4. Immobilization of AAV on the Substrates.** Recombinant AAV r3.45 vectors encoding GFP were adsorbed onto the adhesive pNE or pDA interfaces on TCP substrates. To immobilize the viral vectors,  $5 \times 10^9$  viral genomic (vg) particles in PBS/0.01% Tween 20 were loaded onto the pNE- or pDA-coated substrates by gentle agitation for 12 h at 37 °C. Loosely bound AAV vectors were removed by gently rinsing two times with PBS/0.01% Tween 20. For controls, AAV r3.45 vectors were adsorbed onto unmodified TCPs. The quantity of the resulting vectors immobilized on each substrate (unmodified TCP and pDA- and pNE-coated substrates) was determined using qPCR analysis.

### 2.5. Characterization of AAV\_pNE or AAV\_pDA Interfaces.

The topographical morphologies of the catecholamine-coated interfaces and AAV-bound substrates were visualized using atomic force microscopy (AFM) (AFM; Dimension 3100 SPM with a Nanoscope IV, Digital Instruments, Santa Barbara, CA). To analyze the release kinetics of surface-bound AAV vectors, Alexa Fluor 594 dye (Invitrogen) was tagged to the AAV vectors using a microscale protein labeling kit (Invitrogen), and the fluorescently labeled AAV r3.45 vectors on each substrate were incubated in PBS at 37 °C. At designated time points (4, 48, 96, and 144 h), the supernatant was collected, and the fluorescence intensity of the supernatant at each time point was quantified using a spectrophotometer (Nanodrop 2000, Thermo Scientific, West Palm Beach, FL, USA). The fluorescence intensity at each time point was normalized to the fluorescence intensity of the initial quantity. Cumulative AAV release from each substrate at each time point was determined to be the total viral quantity released until the designated time point. Viral genomic (vg) particles were calculated based on the percentage obtained after normalization. To examine the adhesive force of sticky catecholamines from the TCP substrate, pull-off forces were measured using the Universal Micro-Tribometer (UMT; TopTac2000, Yeonjin Corporation, Korea). A constant force (100g) was applied to all substrates (nonmodified TCP and pDA- and pNE-coated TCPs) for 5 s. Subsequently, the pull-off forces were measured by withdrawing the stage in a vertical direction at a velocity of 100 μm/s. All the forces are defined as the pull-off force (μN) divided by the exerted unit area (cm<sup>2</sup>). All applied forces were normalized to the pull-off force obtained from the nonmodified TCP substrate.

**2.6. Transduction Assay.** To test cellular transduction, hNSCs were plated onto 48-well tissue culture plates (TCPs) at a density of  $1 \times 10^5$  cells/well immediately after immobilizing AAV r3.45 vectors onto the adhesive pNE- or pDA-coated substrates. The cell culture medium was replaced at 12 h post-transduction, and the cells were

cultured for an additional 18, 24, 48, or 96 h before analysis. To examine the cellular transduction ability of AAV r3.45 vectors immobilized on sticky substrates, two control conditions were utilized: (i) hNSCs were plated onto the 48-well TCPs containing AAV r3.45 vectors nonspecifically bound on the substrate without the pNE or pDA coating and (ii) hNSCs were seeded onto the 48-well TCPs, and AAV r3.45 vectors ( $5 \times 10^9$  genomic particles) were directly added on top of the medium for bolus delivery. The bolus delivery refers to the direct addition of AAV vectors ( $5 \times 10^9$  vg) at the same concentration as the initial viral quantity used for surface immobilization. For bolus delivery, hNSCs were simply fed with fibroblast growth factor-2 (FGF-2) supplemented medium every other day to maintain AAV vectors in the medium. The viral genomic multiplicity of infection (MOI; viral genomic particles/cell) for all conditions was 50 000. Additionally, to expand its application, pNE and pDA were coated on glass and poly(caprolactone) (PCL) electrospun fibrous scaffolds (15% (w/v) PCL in chloroform:dimethylformamide (8:2), at a 12 cm distance, 12.4 kV), and hNSCs were transduced using the same procedures. Transduction efficiency was quantified by flow cytometry at the Yonsei University College of Medicine Medical Research Center (Becton Dickinson FACS-Calibur, Franklin Lakes, NJ), and the percentage of cells expressing GFP was quantified to determine cellular transduction efficiency.

**2.7. Internalization of AAV Vectors Delivered from pNE- or pDA-Interfaces.** AAV r3.45 vectors fluorescently labeled with Alexa Fluor 594 were immobilized onto TCP substrates coated with pNE (2 and 0.02 mg/mL), and hNSCs were subsequently plated onto the substrates. At designated times after exposure to the surface-bound AAV vectors (2, 4, 6, 10, 18, and 24 h), the cells were trypsinized, replated onto new 48-well TCPs, and grown for an additional 12 h prior to fluorescence imaging. This procedure was performed to remove the surface-associated viral vectors and limit the analysis to AAV vectors internalized across the cellular membrane by imaging only fluorescently labeled AAV r3.45 vectors within the cytoplasm (Eclipse Ti-S, Nikon, Tokyo, Japan).

**2.8. Analysis of Vector Delivery Mechanisms.** To investigate different vector delivery mechanisms, the receptor-mediated delivery of AAV vectors was inhibited by removing glycosaminoglycans (GAG) on the cell membrane, including heparan sulfate and chondroitin sulfate, and gene delivery efficiency (e.g., GFP expression) was examined. Prior to cellular transduction, hNSCs were incubated for 90 min with either 5 units/mL of chondroitinase ABC (Sigma-Aldrich) or 2 units/mL of heparinase II (Sigma-Aldrich) dissolved in PBS supplemented with 10% bovine serum albumin (BSA). Then, hNSCs were transduced with AAV r3.45 vectors. Finally, the GAG-mediated AAV delivery mechanism was analyzed by quantifying the percentage of GFP-expressing cells with and without GAG lyase treatment.

**2.9. Cytotoxicity Test.** To test the cytotoxicity of the pNE- or pDA-mediated AAV delivery system, the metabolic activity of transduced hNSCs was quantified by colorimetric measurement using a WST-1 assay kit (Roche Applied Science, Indianapolis, IN, USA). Briefly, hNSCs were plated on 48-well plates ( $1 \times 10^5$  cells/well), transduced with AAV r3.45 vectors delivered via different routes (bolus, nonmodified surfaces, and pDA- or pNE-substrates), and harvested at 2 days post-transduction. Subsequently, 0.1 volume of WST-1 solution (1/10 of the original culture medium) was directly added to each well and incubated for an additional 4 h at 37 °C. The supernatants were collected, and the colorimetric changes at 450 nm were measured using a spectrophotometer (Nanodrop 2000, Thermo Scientific, West Palm Beach, FL, USA). Finally, absorbance values for each condition were normalized to the absorbance value of a control condition in which cells were cultured for 2 days on the unmodified TCPs without AAV transduction.

**2.10. Proliferation of hNSCs by the Sticky Interface-Mediated AAV Delivery.** To evaluate the sticky interface-mediated AAV delivery system as a platform to induce physiological responses by hNSCs, we measured hNSC proliferation. Recombinant AAV r3.45 vectors encoding fibroblast growth factor-2 (FGF-2) (AAV-FGF2) driven by a CMV promoter were packaged and purified according to

the method used to package AAV-GFP. Cellular proliferation assays were performed under the following conditions: (i) hNSC culture on the nonmodified TCPs with or without FGF, (ii) bolus delivery of AAV-FGF2 or AAV-GFP without FGF supplement, (iii) pDA-mediated delivery of AAV-FGF2 or AAV-GFP without FGF supplement, and (iv) pNE-mediated delivery of AAV-FGF2 or AAV-GFP without FGF supplement. hNSC proliferation was analyzed using an alamar blue assay kit (Invitrogen). Briefly, hNSCs were transduced with AAV r3.45 vectors ( $5 \times 10^9$  vg) encoding FGF-2 and grown in 48-well plates. After 4 days in culture, 15  $\mu$ L of alamar blue (Invitrogen) was directly added to each well, and the cells were incubated at 37 °C for another 24 h. Colorimetric changes were detected at 570 nm using a spectrophotometer (Nanodrop 2000, Thermo Scientific, West Palm Beach, FL, USA) and normalized to the negative control (hNSC culture on the unmodified TCP without FGF-2 protein supplement).

**2.11. Statistics.** All of the experiments were performed in triplicate, and the experimental data are presented as the mean  $\pm$  the standard deviation (SD). Statistical significance was determined using one-way analysis of variance (ANOVA) with a post hoc Dunnett's test, and all calculations were performed using the SPSS (Statistical Package for the Social Sciences) 18.0 software package (IBM Corporation, Somers, NY, USA).

### 3. RESULTS AND DISCUSSION

As illustrated in Figure 1, AAVr3.45 vectors that specifically target hNSCs were combined with adhesive pNE- or pDA-

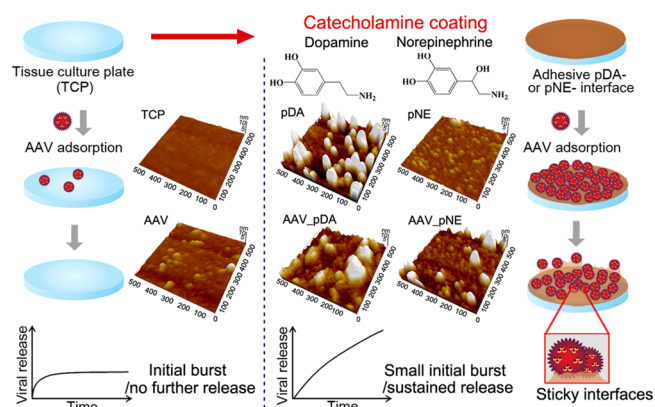


**Figure 1.** Formulation of adhesive pNE and pDA interfaces containing adsorbed AAV vectors. The catecholamine interfaces were formulated by polymerizing each monomer under alkaline conditions. The topographies of various surfaces with or without AAV adsorption were visualized by atomic force microscopy (AFM) analysis, including an unmodified polystyrene tissue culture plate (TCP) and pNE- and pDA-interfaces (0.02 mg/mL).

interfaces to develop highly versatile “delivering-from” approaches. Viral vectors adsorbed onto unmodified tissue culture plates (TCPs), which weakly interact with the surfaces, may be irregularly or rapidly dissociated from surfaces for subsequent slow release. In contrast, the adhesiveness of pNE- or pDA-interfaces served as a primary factor to retard viral release, preventing initial burst and progressively releasing vectors at a fixed rate (Figure 1). Anchoring AAVr3.45 vectors on sticky pNE- or pDA-coated substrates resulted in approximately 85–99% or 69–78% viral immobilization, respectively, whereas only 24% of the applied viral vectors were immobilized on unmodified TCP (Figure 2A). These percentages indicate the ratio of surface-bound AAV to the initial amount ( $5 \times 10^9$  viral genomic (vg) particles) used for surface immobilization. The pNE interface induced better viral

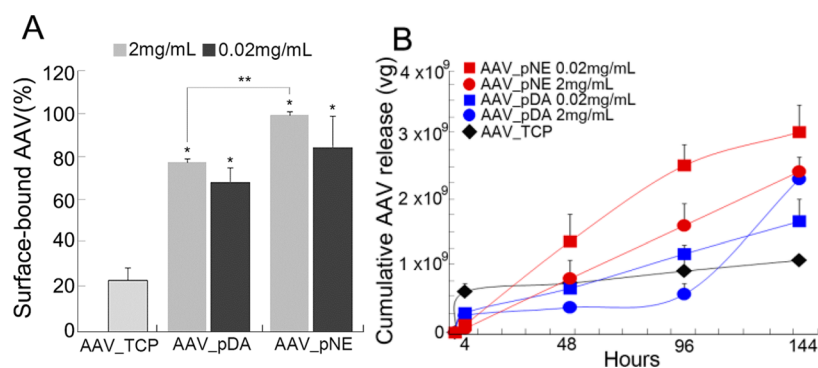


**Figure 2.** AAV immobilization and release from sticky interfaces. (A) The quantity of surface-bound AAVr3.45 vectors as a function of catecholamine concentrations (2 and 0.02 mg/mL). Genomic particles adsorbed on the surface were measured using qPCR analysis and normalized to the initial amount of genomic particles used for surface immobilization. The symbol \* indicates a significant difference compared to the AAV quantity on the unmodified AAV\_TCP ( $P < 0.01$ ). \*\* Indicates a significant difference ( $P < 0.05$ ). (B) The cumulative quantities of AAVr3.45 released from each substrate at 4, 48, 96, and 144 h. The fluorescence intensity of fluorescently labeled AAV vectors collected in the supernatant at each time point was measured using a spectrophotometer and normalized to the initial value. The number of viral genomic (vg) particles released at each time point was calculated based on the percentages.

immobilization than pDA, and the quantity of AAV on the pNE interface formed using the 0.02 mg/mL concentration was larger than that adsorbed on the pDA interface using 2 mg/mL DA. This observation might be explained by the fact that pNE displayed less aggregation and uniform spreading, as confirmed by atomic force microscopy (AFM) (Figure 1 and Supporting Information (SI) Figure S1). Interestingly, the extent of adhesiveness of the pNE surfaces ( $0.190\text{--}0.243 \mu\text{N}/\text{cm}^2$ ), which was defined as pull-off forces ( $\mu\text{N}$ ) divided by the exerted unit area ( $\text{cm}^2$ ), was significantly greater than those of the pDA surfaces ( $0.168\text{--}0.183 \mu\text{N}/\text{cm}^2$ ) (SI Figure S2) due to the additional alkyl hydroxyl group in NE.<sup>15,16</sup>

Importantly, distinct vector release profiles from each substrate were observed, depending upon the interface types and the concentration of catecholamines (Figure 2B). Over 70% of the attached AAV was burst released from the unmodified TCP within 4 h (black line), whereas the adhesive interfaces exhibited sustained release of viral vectors, without initial burst during the early stage ( $< 4$  h) (red line: pNE; blue line: pDA). The pNE surface produced an ideal constant release profile from the start of release to 144 h ( $1.72 \times 10^7$  vg/hours for 2 mg/mL and  $2.14 \times 10^7$  vg/hours for 0.2 mg/mL of coating condition), with a narrow standard deviation (red line). The observed sustained release results from the even distribution of viral vectors for exposure to the external environment, while the sticky properties of pNE prevent initial burst release. pNE-modified substrate with higher pull-off forces (SI Figure S2) slowed the viral release rate (2 mg/mL of pNE  $< 0.02$  mg/mL pNE), suggesting that the stickiness of surfaces, mediated by the type and density of catecholamines, could be a key factor for modulating AAV release.

Prior to examining cellular transduction, the metabolic activity and cell adhesion on the sticky surfaces containing AAVr3.45 vectors were examined. Cellular viability on the catecholamine-interfaces was slightly or significantly improved compared with all the other modes of delivery (SI Figure S3). Sticky surfaces with AAV vectors generally increased cell viability compared to the nonadhesive TCP substrate. The increase in cell viability observed with the sticky interfaces might result from enhanced cellular adhesion relative to unmodified, native substrates (SI Figure S4). The intimate interactions between sticky surfaces and various proteins on the plasma membrane or their ability to protect cellular receptors

from denaturation after substrate contact may trigger cellular adhesion and cell–cell interactions that are crucial for cell survival and metabolic activation.<sup>18</sup>

Sustained release from the sticky interfaces at constant rates without an initial burst significantly enhanced gene delivery efficiency compared to bolus or unmodified TCP-mediated delivery (Figure 3A and B). Bolus delivery refers to the direct

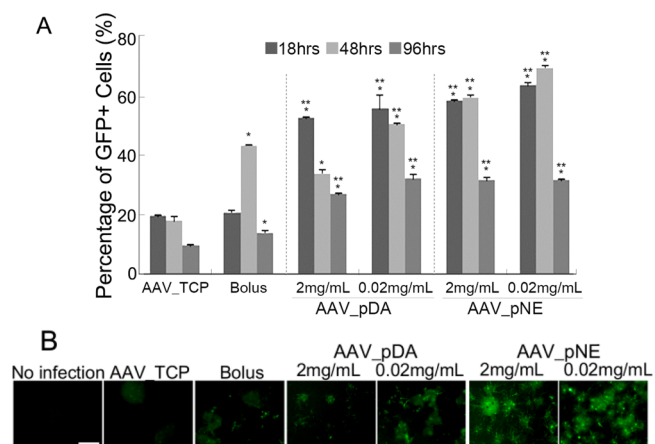


**Figure 3.** Cellular transduction of hNSCs using each delivery mode. (A) The percentage of GFP-expressing cells relative to the total number of hNSCs for each delivery mode at 18, 48, and 96 h post-transduction; \* and \*\* indicate significant differences compared to AAV\_TCP and bolus delivery ( $P < 0.05$ ). (B) Representative fluorescence images of GFP-expressing hNSCs at 48 h post-transduction. The scale bar indicates  $100 \mu\text{m}$ .

addition of AAV vectors ( $5 \times 10^9$  vg) at the same initial viral quantity used for surface immobilization. The gradual AAV release from the pNE and pDA sticky surfaces with fixed rates produced high GFP percentages (58.1–63.4% and 52.4–55.7%, respectively), even at the early times (18 h), whereas both bolus and unmodified TCP-mediated delivery produced approximately 20% GFP-expressing cells at 18 h post-transduction (Figure 3A). pNE interfaces (0.02 mg/mL) displayed the highest delivery efficiency (69.7%) at 2 days post-transduction compared to other delivery modes (Figure 3A and B). The sustained release of AAV vectors from the pNE interfaces (0.02

mg/mL) appears to be efficient compared to that from the pDA interfaces coated with the same density (0.02 mg/mL). As shown in Figure 2B, the persistent release of AAV vectors with larger quantities on the pNE interfaces over the time period might result in more enhanced gene delivery efficiencies than on the pDA interfaces, where lower cumulative AAV releases until 96 h were observed. Additionally, as demonstrated in the AFM images of AAV immobilizations on each interface (Figure 1), more dispersion of AAV vectors on the pNE interfaces, possibly resulting from the improved coating capability of pNE relative to pDA,<sup>16</sup> might facilitate the uptake of viral vectors by a relatively large number of cells. Large portions of AAV aggregations on the pDA interfaces might not only inhibit the cellular internalization of viral vectors, but also provide few chances to deliver genes to a large number of cells, thereby lowering gene delivery efficiencies on pDA interfaces (0.02 mg/mL) compared to pNE interfaces (0.02 mg/mL).

The release profiles and GFP percentages imply that gradual vector exposure at a constant rate is critical for efficient gene delivery to target cells that are stably adhered to substrates. The substantial drops in GFP percentages at 96 h post-transduction may be due to the detachment of hNSCs from the surface and the formation of neurospheres, which were normally observed after 2 days in culture.<sup>26</sup> The separation of hNSCs from the surface might dramatically reduce their physical contact with AAV vectors, especially for cells in the inner spaces of neurospheres, thereby resulting in significant decreases in gene expression at 96 h post-transduction. Adherent cells (i.e., HEK293T) were cultured on the sticky catecholamine substrates containing AAV vectors to prove the crucial role of persistent viral contacts with target cells for promoting gene delivery efficiencies (SI Figure S5). Consequently, sustained AAV release from the pNE or pDA substrates significantly enhanced gene delivery efficiencies in HEK293T cells compared to bolus delivery over the time period. Importantly, the duration of enhanced GFP percentages on the sticky substrates extended until 96 h post-transduction, while gene expression by bolus delivery did not increase after 48 h. The extended duration of gene expression in adherent cells further supports the conclusion that the sustained contact of gene vectors with target cells over the time periods is highly critical to significantly enhance gene delivery. Most importantly, the substantial enhancement of gene delivery efficiencies on the sticky pNE or pDA interfaces in both cell types is evidence of the potential of the catecholamine interfaces as platform tools to efficiently deliver genes of interest toward target cells.

Even with reduced viral quantities (85% and 69%, respectively) on the sticky interfaces compared to bolus delivery (100%) (Figure 2A), the sticky interfaces increased GFP expression by 1.5–3-fold over the course of this experiment ( $P < 0.05$ ) (Figure 3A). Gene delivery efficiency on the unmodified TCP gradually declined (19.2–9.4%) with time. The sticky interfaces were expanded to different substrates, namely, glass and poly(caprolactone) (PCL)-electrospun fibers. Substantially more GFP-expressing cells were observed on the pNE- or pDA-coated glass and PCL fibers than on the unmodified surfaces or following bolus delivery (SI Figure S6), confirming that the material-independent properties of interfaces promote efficient gene delivery.

The gradual release of virus from sticky surfaces at a constant rate resulted in rapid viral internalization across the hNSC membrane (Figure 4A). In cells exposed to fluorescently

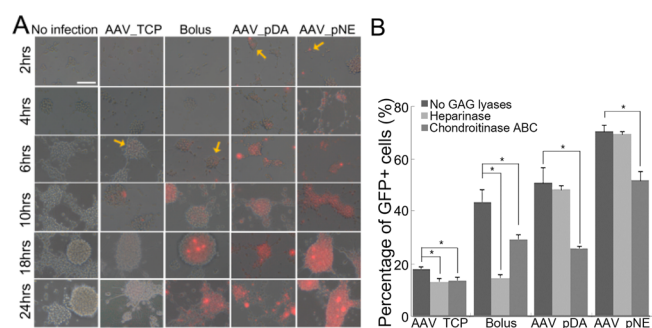


**Figure 4.** Investigation of delivery mechanisms. (A) Cellular internalization of fluorescently labeled AAVr3.45 vectors (red). The fluorescence images were overlaid with phase-contrast images of hNSCs. The scale bar indicates 100  $\mu$ m. The yellow arrows indicate the internalized vectors. (B) The effect of GAGs on cellular transduction. The percentages of GFP-expressing cells measured with and without the GAG lyases were quantified to compare delivery mechanisms. \* Indicates a significant difference ( $P < 0.05$ ).

labeled vectors on sticky surfaces, we observed fluorescence expression within 2 h, whereas cells transduced by bolus delivery or on unmodified TCP exhibited only faint fluorescence at 6 h post-transduction. In the bolus delivery system, strong fluorescence was not observed until 24 h post-transduction. The sticky surfaces might coordinate robust interactions between hNSCs and the viral vectors that were progressively supplied to the cellular microenvironment, ultimately leading to fast and efficient gene delivery.

Next, we sought to determine the mechanism by which sticky interfaces enhance gene delivery. Glycosaminoglycans (GAGs), such as heparan sulfate proteoglycan (HSPG) and chondroitin sulfate proteoglycans (CSPGs), which mediate various signal networks in neural stem cells,<sup>28</sup> were removed at the cell surface by treatment with chondroitinase ABC or heparinase II prior to gene delivery. In a bolus or unmodified TCP-mediated delivery, the removal of these GAGs significantly reduced delivery efficiency, suggesting that these GAGs function as primary receptors for AAVr3.45 in hNSCs (Figure 4B). Although the removal of CSPGs substantially affected the delivery efficiency of sticky interfaces, as was observed for other modes, defects in HSPGs did not inhibit sticky surface-mediated delivery. These findings suggest that sustained contact of vectors with hNSCs can bypass HSPG pathways. Figure 4B also implies that finding a novel means to closely interact with CSPGs can be a key clue to further enhance gene delivery efficiencies for hNSC.

Finally, sticky interfaces were evaluated as ex vivo platforms for inducing physiological responses in hNSCs, such as proliferation, which was stimulated by AAVr3.45 encoding for fibroblast growth factor-2 (FGF-2) (Figure 5). The expression of FGF-2 is required for maintaining multipotency and inducing proliferation in NSCs.<sup>29</sup> To form sticky surfaces, we used the catecholamine concentration (0.02 mg/mL) that resulted in the highest GFP expression (Figure 3A) in our previous experiments. The level of hNSC proliferation stimulated by FGF-2 expression in cells transduced with AAVr3.45-FGF2 on the pNE interface was better than that induced by normal proliferation conditions (20 ng/mL FGF-2 protein supplement on alternate days) (Figure 5A and B). pDA-mediated delivery significantly enhanced proliferation compared to negative controls and bolus delivery, but it also significantly reduced proliferation compared to the positive

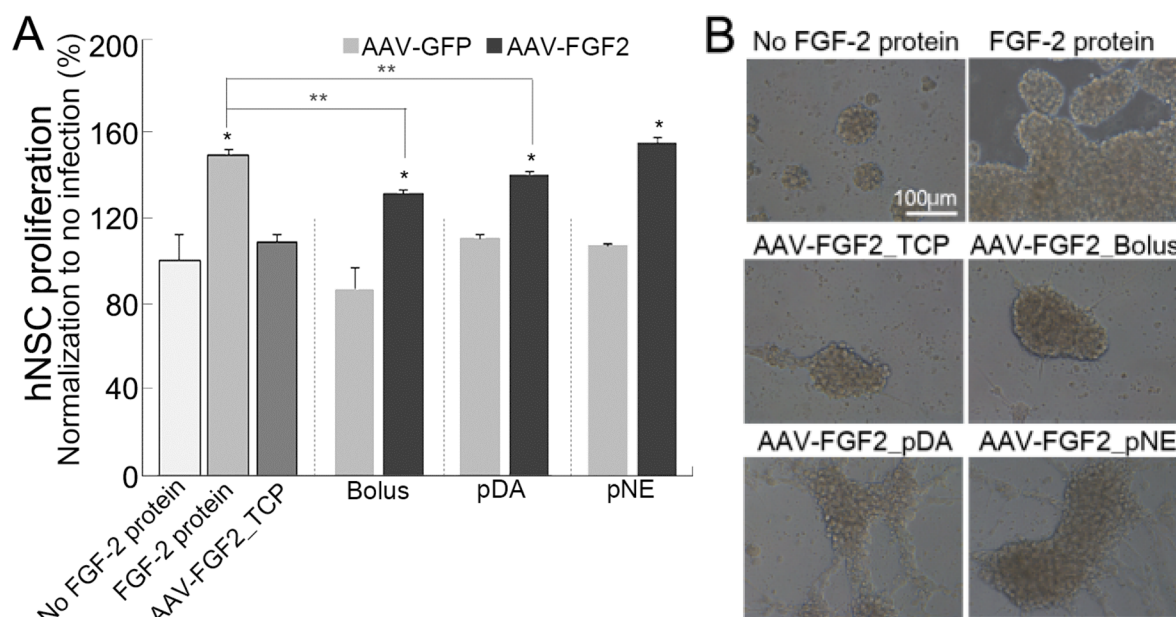


**Figure 5.** Physiological responses of hNSCs to AAV-FGF delivery from sticky interfaces. (A) Proliferation of hNSCs was measured using the alamar blue assay at 4 days post-transduction. The normal hNSC culture condition (supplementation of 20 ng/mL FGF-2 on alternate days) was used as a positive control, and the following negative controls were used: no FGF-2 treatment in medium and AAV-GFP delivery; \* and \*\* indicate significant differences compared to the negative and positive control, respectively ( $P < 0.05$ ). (B) Representative phase-contrast images of hNSCs stimulated by each delivery mode at 4 days post-transduction.

control. A single-shot of AAV-FGF2 from sticky interfaces was sufficient to induce hNSC proliferation, a physiological response that is typically achieved by multiple treatments with expensive FGF-2 proteins. Thus, these data demonstrate that sticky interfaces represent powerful ex vivo toolboxes that can be extensively used in gene therapy or stem cell applications.

#### 4. CONCLUSIONS

In conclusion, this study is the first to employ bioinspired catecholamines as viral vector carriers to efficiently deliver genes of interest to clinically valuable cell types, specifically hNSCs. The material-independent properties of pNE and pDA suggest that they might be useful for numerous biomedical applications. The successful establishment of sticky “delivering-from” systems that can efficiently tune viral release at fixed rates and induce gene expression in a controlled manner will validate the development of “smart” gene delivery systems using sticky catecholamines.

#### ■ ASSOCIATED CONTENT

##### Supporting Information

Supplementary figures: the topographies of various surfaces with or without AAV vectors (Figure S1), the adhesive properties of catecholamine interfaces (i.e., pull-off forces) (Figure S2), the viability of hNSCs (Figure S3), hNSC adhesion on each substrate (Figure S4), cellular transduction of HEK293T cells using each delivery mode (Figure S5), and cellular transduction of hNSCs on glass surfaces and PCL electrospun fibers (Figure S6). This material is available free of charge via the Internet at <http://pubs.acs.org>.

#### ■ AUTHOR INFORMATION

##### Corresponding Author

\*E-mail: [j-jang@yonsei.ac.kr](mailto:j-jang@yonsei.ac.kr).

#### Author Contributions

The manuscript was written through contributions of all authors. All authors have given approval to the final version of the manuscript.

#### Notes

The authors declare no competing financial interest.

#### ■ ACKNOWLEDGMENTS

This work was supported by the National Research Foundation of Korea (NRF) grant through the Active Polymer Center for Pattern Integration (2007-0056091, J.-H. J.), Basic Science Research Program (2012R1A1A1003397, J.-H. J.), and Bio & Medical Technology Development Program (2013M3A9D3045879, J.-H.J. and 2012-0006085, H.L.) funded by the Ministry of Science, ICT & Future Planning (MSIP).

#### ■ REFERENCES

- (1) Jang, J. H.; Schaffer, D. V.; Shea, L. D. Engineering Biomaterial Systems to Enhance Viral Vector Gene Delivery. *Mol. Ther.* **2011**, *19*, 1407–1415.
- (2) Jang, J. H.; Houchin, T. L.; Shea, L. D. Gene Delivery from Polymer Scaffolds for Tissue Engineering. *Expert Rev. Med. Devices* **2004**, *1*, 127–138.
- (3) Pannier, A. K.; Shea, L. D. Controlled Release Systems for DNA Delivery. *Mol. Ther.* **2004**, *10*, 19–26.
- (4) Jang, J. H.; Bengali, Z.; Houchin, T. L.; Shea, L. D. Surface Adsorption of DNA to Tissue Engineering Scaffolds for Efficient Gene Delivery. *J. Biomed. Mater. Res., Part A* **2006**, *77*, 50–58.
- (5) Segura, T.; Volk, M. J.; Shea, L. D. Substrate-Mediated DNA Delivery: Role of the Cationic Polymer Structure and Extent of Modification. *J. Controlled Release* **2003**, *93*, 69–84.
- (6) Hu, W. W.; Syu, W. J.; Chen, W. Y.; Ruaan, R. C.; Cheng, Y. C.; Chien, C. C.; Li, C.; Chung, C. A.; Tsao, C. W. Use of Biotinylated Chitosan for Substrate-Mediated Gene Delivery. *Bioconjugate Chem.* **2012**, *23*, 1587–1599.
- (7) Yuan, W.; Li, C.; Zhao, C.; Sui, C.; Yang, W.-T.; Xu, F.-J.; Ma, J. Facilitation of Gene Transfection and Cell Adhesion by Gelatin-

Functionalized Pcl Film Surfaces. *Adv. Funct. Mater.* **2012**, *22*, 1835–1842.

(8) Li, C. Y.; Yuan, W.; Jiang, H.; Li, J. S.; Xu, F. J.; Yang, W. T.; Ma, J. PCL Film Surfaces Conjugated with P(Dmaema)/Gelatin Complexes for Improving Cell Immobilization and Gene Transfection. *Bioconjugate Chem.* **2011**, *22*, 1842–1851.

(9) Shin, S.; Salvay, D. M.; Shea, L. D. Lentivirus Delivery by Adsorption to Tissue Engineering Scaffolds. *J. Biomed. Mater. Res., Part A* **2010**, *93*, 1252–1259.

(10) Gu, D. L.; Nguyen, T.; Gonzalez, A. M.; Printz, M. A.; Pierce, G. F.; Sosnowski, B. A.; Phillips, M. L.; Chandler, L. A. Adenovirus Encoding Human Platelet-Derived Growth Factor-B Delivered in Collagen Exhibits Safety, Biodistribution, and Immunogenicity Profiles Favorable for Clinical Use. *Mol. Ther.* **2004**, *9*, 699–711.

(11) Jang, J. H.; Koerber, J. T.; Gujrati, K.; Bethi, S. R.; Kane, R. S.; Schaffer, D. V. Surface Immobilization of Hexa-Histidine-Tagged Adeno-Associated Viral Vectors for Localized Gene Delivery. *Gene Ther.* **2010**, *17*, 1384–1389.

(12) Pandori, M.; Hobson, D.; Sano, T. Adenovirus-Microbead Conjugates Possess Enhanced Infectivity: A New Strategy for Localized Gene Delivery. *Virology* **2002**, *299*, 204–212.

(13) Gersbach, C. A.; Coyer, S. R.; Le Doux, J. M.; Garcia, A. J. Biomaterial-Mediated Retroviral Gene Transfer Using Self-Assembled Monolayers. *Biomaterials* **2007**, *28*, 5121–5127.

(14) Lee, H.; Dellatore, S. M.; Miller, W. M.; Messersmith, P. B. Mussel-Inspired Surface Chemistry for Multifunctional Coatings. *Science* **2007**, *318*, 426–430.

(15) Kang, S. M.; Rho, J.; Choi, I. S.; Messersmith, P. B.; Lee, H. Norepinephrine: Material-Independent, Multifunctional Surface Modification Reagent. *J. Am. Chem. Soc.* **2009**, *131*, 13224–13225.

(16) Hong, S.; Kim, J.; Na, Y. S.; Park, J.; Kim, S.; Singha, K.; Im, G. I.; Han, D. K.; Kim, W. J.; Lee, H. Poly(Norepinephrine): Ultrasoft Material-Independent Surface Chemistry and Nanopotential for Nitric Oxide. *Angew. Chem., Int. Ed.* **2013**, *52*, 9187–9191.

(17) Jang, J. H.; Koerber, J. T.; Kim, J. S.; Asuri, P.; Vazin, T.; Bartel, M.; Keung, A.; Kwon, L.; Park, K. I.; Schaffer, D. V. An Evolved Adeno-Associated Viral Variant Enhances Gene Delivery and Gene Targeting in Neural Stem Cells. *Mol. Ther.* **2011**, *19*, 667–675.

(18) Ku, S. H.; Ryu, J.; Hong, S. K.; Lee, H.; Park, C. B. General Functionalization Route for Cell Adhesion on Non-Wetting Surfaces. *Biomaterials* **2010**, *31*, 2535–2541.

(19) Sun, K.; Xie, Y.; Ye, D.; Zhao, Y.; Cui, Y.; Long, F.; Zhang, W.; Jiang, X. Mussel-Inspired Anchoring for Patterning Cells Using Polydopamine. *Langmuir* **2012**, *28*, 2131–2136.

(20) Ryu, J.; Ku, S. H.; Lee, H.; Park, C. B. Mussel-Inspired Polydopamine Coating as a Universal Route to Hydroxyapatite Crystallization. *Adv. Funct. Mater.* **2010**, *20*, 2132–2139.

(21) Garcia-Fernandez, L.; Cui, J.; Serrano, C.; Shafiq, Z.; Gropeanu, R. A.; Miguel, V. S.; Ramos, J. I.; Wang, M.; Auernhammer, G. K.; Ritz, S.; Golriz, A. A.; Berger, R.; Wagner, M.; del Campo, A. Antibacterial Strategies from the Sea: Polymer-Bound Cl-Catechols for Prevention of Biofilm Formation. *Adv. Mater.* **2013**, *25*, 529–533.

(22) You, L.; Kang, S. M.; Lee, S.; Cho, Y. O.; Kim, J. B.; Lee, S. B.; Nam, Y. S.; Lee, H. Polydopamine Microfluidic System toward a Two-Dimensional, Gravity-Driven Mixing Device. *Angew. Chem., Int. Ed.* **2012**, *51*, 6126–6130.

(23) Liu, Q.; Yu, B.; Ye, W.; Zhou, F. Highly Selective Uptake and Release of Charged Molecules by Ph-Responsive Polydopamine Microcapsules. *Macromol. Biosci.* **2011**, *11*, 1227–1234.

(24) Kong, J.; Yee, W. A.; Yang, L.; Wei, Y.; Phua, S. L.; Ong, H. G.; Ang, J. M.; Li, X.; Lu, X. Highly Electrically Conductive Layered Carbon Derived from Polydopamine and Its Functions in SnO<sub>2</sub>-Based Lithium Ion Battery Anodes. *Chem. Commun. (Camb.)* **2012**, *48*, 10316–10318.

(25) Li, R.; Parvez, K.; Hinkel, F.; Feng, X.; Mullen, K. Bioinspired Wafer-Scale Production of Highly Stretchable Carbon Films for Transparent Conductive Electrodes. *Angew. Chem., Int. Ed.* **2013**, *52*, 5535–5538.

(26) Kim, H. T.; Kim, I. S.; Lee, I. S.; Lee, J. P.; Snyder, E. Y.; Park, K. I. Human Neurospheres Derived from the Fetal Central Nervous System Are Regionally and Temporally Specified but Are Not Committed. *Exp. Neurol.* **2006**, *199*, 222–235.

(27) Koerber, J. T.; Maheshri, N.; Kaspar, B. K.; Schaffer, D. V. Construction of Diverse Adeno-Associated Viral Libraries for Directed Evolution of Enhanced Gene Delivery Vehicles. *Nat. Protoc.* **2006**, *1*, 701–706.

(28) Yu, R. K.; Yanagisawa, M. Glycosignaling in Neural Stem Cells: Involvement of Glycoconjugates in Signal Transduction Modulating the Neural Stem Cell Fate. *J. Neurochem.* **2007**, *103* (Suppl 1), 39–46.

(29) Reynolds, B. A.; Weiss, S. Generation of Neurons and Astrocytes from Isolated Cells of the Adult Mammalian Central Nervous System. *Science* **1992**, *255*, 1707–1710.